The vibrational density of states of a disordered gel model

Lorenzo Rovigatti, Walter Kob, and Francesco Sciortino

Citation: J. Chem. Phys. **135**, 104502 (2011); doi: 10.1063/1.3626869
View online: http://dx.doi.org/10.1063/1.3626869
View Table of Contents: http://jcp.aip.org/resource/1/JCPSA6/v135/i10
Published by the American Institute of Physics.

The vibrational density of states of a disordered gel model

Lorenzo Rovigatti,[1,a)] Walter Kob,[2] and Francesco Sciortino[3]
[1]*Dipartimento di Fisica, Università di Roma La Sapienza, Piazzale A. Moro 2, 00185 Roma, Italy*
[2]*Laboratoire Charles Coulomb, Université Montpellier 2, CNRS UMR 5221, 34095 Montpellier, France*
[3]*Dipartimento di Fisica and CNR-ISC, Università di Roma La Sapienza, Piazzale A. Moro 2, 00185 Roma, Italy*

(Received 19 May 2011; accepted 2 August 2011; published online 9 September 2011)

We investigate the vibrational density of states (vDOS) in harmonic approximation of a binary mixture of colloidal patchy particles with two and three patches for different relative compositions x_2. At low temperature, this system forms a thermo-reversible gel, i.e., a fully bonded network of chains of two-patches particles, in which the branching points are provided by three-patches particles. For all the compositions, we find in the vDOS a pronounced peak at low frequency whose height grows on increasing the fraction of two-functional particles or equivalently with the average length of the chains. To identify the various spectral features, we compare the vDOS of the whole system with the one of small representative structures of the network and with the vDOS of a long linear chain of two-patches particles and we find that these structures are indeed able to rationalize the various peaks in the vDOS of the full system. At large x_2 the vDOSs of the gel and of the long chain show remarkable similarities. Analyzing the dispersion relations and the spectrum of the linear chain we show that the excess of low frequency modes, the analog of the boson peak in glassy disordered systems, arises from the strong coupling between rotations and translations. © *2011 American Institute of Physics*. [doi:10.1063/1.3626869]

I. INTRODUCTION

The study of the vibrational density of states (vDOS) is central in the investigation of solids,[1,2] since, apart from the structure, it is probably the most relevant and direct quantity to characterize a system. For example, within the harmonic approximation, the vDOS (which we will denote by $g(\omega)$, where ω is the frequency), allows one to calculate the temperature dependence of the specific heat, thermal conductivity, as well as the free energy. It has been known for a long time that the vDOS of *disordered* systems shows anomalies that have features which are not observed in crystalline systems. A well-known example is the vDOS of fractal aggregates for which one finds that $g(\omega)$ shows at low ω a power-law dependence with a fractal exponent, instead of the typical Debye law ω^{d-1}, where d is the dimensionality of space.[3–5] Deviations from the Debye law are also often observed in atomic and molecular glasses and have been in the focus of interest of many studies.[6–20] The most remarkable anomaly is an excess in the number of modes, as compared to the Debye prediction, at low frequencies (i.e., for an atomic system in the THz range), a feature which is commonly named "boson peak" and which is responsible for the anomalous behavior in the specific heat or thermal conductivity of glasses.[9,12,13,19] Although some evidence has been provided for the existence of a correlation between the fragility of a glass-forming system and the strength of its boson peak, other results suggest that no such correlation exists.[7,21,22] It has been proposed that this correlation has a structural origin,[20,21] since strong glass-formers have an open network structure (due to the presence of directional/ionic bonds) and tend to have a strong boson peak, while fragile liquids have a structure that is similar to the one of the hard sphere systems, i.e., van der Waals like interactions, and usually a weak boson peak. Similar results have been found in the Se_xAs_{1-x} system for which neutron scattering shows that the number of low frequency modes is related to the average coordination number of the atoms.[23]

While much effort has been devoted to the investigation of dense glasses, much less is known for the case of thermoreversible gels, i.e., disordered arrested states at low densities.[24] One of the reasons for this is that the realistic modeling of thermoreversible gels has become possible only recently.[25–31] Models include patchy particles of low valence, particles interacting via competing short- and long-range interactions, three-body potentials, dipolar particles, and others.[24] In all these models, the interaction potential makes that the particles have only a small coordination number which in turn allows to generate very open disordered structures, composed by chains of bi-coordinated particles joined by a small number of three- (or more) coordinated particles which act as junctions in the network. In the last years, the structural and relaxational properties of these thermoreversible gel models have been extensively investigated in the attempt to deepen our understanding of the mechanisms responsible for the slowing down of the dynamics with decreasing temperature and to clarify the differences between gels and glasses.[24]

In the present work, we extend this line of investigations and focus on the vDOS of one of these models, a binary mixture of particles with, respectively, two and three attractive patches. By changing the relative composition of the mixture, we can change in a controlled way the structural properties of the system[32] and, in particular, the length of the bi-functional

a)Author to whom correspondence should be addressed. Electronic mail: lorenzo.rovigatti@uniroma1.it.

chains connecting the three-functional particles. This flexibility will allow us to study how a change of the structure influences the properties of the vDOS as well as the behavior of the system at low frequencies, where a strong coupling between rotational and translational degrees of freedom is found.

II. MODEL AND COMPUTATIONAL DETAILS

The model used in the present study has been presented in detail in Ref. 32. Hence, we provide here only the necessary amount of information required to make the article self-contained.

A. The interaction potential

The particles are modeled as spherical rigid bodies of diameter σ and mass m. The surface of particle i is decorated with M_i sticky spots called patches. These patches are located at a distance $\sigma/2$ from the particle's center of mass. The total interaction between particles i and j is

$$V(i,j) = V_{\mathrm{CM}}(i,j) + V_P(i,j), \tag{1}$$

where V_{CM} is the interaction between the centers of mass of the two particles, while V_P is the potential acting between the patches. So the total potential of the system is $V_{tot} = \sum_{i,j} V(i,j)$. We have chosen

$$V_{\mathrm{CM}}(i,j) = \left(\frac{\sigma}{r_{ij}}\right)^{200} \tag{2}$$

and

$$V_P(i,j) = -\epsilon \sum_{p=1}^{M_i}\sum_{q=1}^{M_j} \exp\left[-\frac{1}{2}\left(\frac{r_{ij}^{(pq)}}{0.12\sigma}\right)^{10}\right], \tag{3}$$

where r_{ij} is the distance between the centers of mass of particles i and j and $r_{ij}^{(pq)}$ is the distance between patch p on particle i and patch q on particle j. With this choice of parameters, the resulting potential resembles a hard sphere potential complemented by an attractive square well-like potential if patches on different particles are close to each other. In addition, the very short range of V_P guarantees that the so-called "single bond per patch condition" is fulfilled. This condition means that the maximum number of possible bonds that particle i can form is equal to M_i, and it allows to make an analytical description of the structural and dynamical properties of the model.[27,33,34] By choosing $\epsilon = 1.001$, one finds that the depth of the $V(i,j)$ potential is $u_0 = 1.0$.

B. Details of the simulations

The studied system is a binary mixture of N_2 bi-functional particles, $M_i = 2$, and N_3 three-functional particles, $M_j = 3$, with $N \equiv N_2 + N_3 = 1000$ at packing fraction $\phi = (\pi/6)(\sigma^3 N/V) = 0.1$, where V is the total volume of the system. Patches are arranged on the poles for particles with two patches (bi-functional particles) and equally spaced on the equator for particles with three patches (three-functional particles). We have studied six different systems having the following concentrations of bi-functional particles $x_2 \equiv N_2/N$: 0.2, 0.5, 0.66, 0.75, 0.85, and 0.9. This gives us the possibility to investigate how the average valence $\overline{M} \equiv 3 - x_2$ influences the structure and the vibrational properties of the system. In the following, energy is measured in units of u_0, distance in units of σ, and time in units of $\sqrt{m\sigma^2/\epsilon}$. Temperature, T, is measured in units of energy, setting the Boltzmann constant $k_B = 1$.

The configurations we analyze were generated via Brownian dynamics[32] by equilibrating the systems at $T = 0.055$ (a T at which essentially most of the possible bonds have already been formed) and by quenching the final equilibrium configurations to $T = 0.04$. The simulation at $T = 0.04$ is performed until the few remaining isolated monomers attach to the spanning cluster. Indeed, at such a low temperature, the probability of breaking a bond, proportional to $e^{-1/k_B T}$, is of the order of 10^{-11} and hence no bond breaking occurs during the simulation ($\sim 10^8$ time steps, where each time step corresponds to $\delta t = 0.001$). We stress that, in the resulting structure, all the particles belong to the same cluster and the connectivity of the system is not altered by the dynamics, i.e., in the following we study only the vibrational dynamics and not the relaxation and thus the system can be considered as a chemical gel. Note that this vibrational dynamics is not harmonic since the system is able to overcome local barriers, but which are not associated with bond breaking events.

C. Method to evaluate the harmonic density of states

We have computed the normal modes and eigenfrequencies of the system by determining the properties of the local potential energy minimum configuration $\mathbf{q}^*$, i.e., a configuration for which $\nabla_{\mathbf{q}} V_{tot}(\mathbf{q})|_{\mathbf{q}^*} = \mathbf{0}$, where $\mathbf{q}$ are the generalized coordinates (center of mass positions and orientational angles). This local minimum was obtained by taking a configuration of the system as a starting point of a minimization procedure in the potential energy V_{tot} and the so obtained local minimum is $\mathbf{q}^*$. Note that this minimum configuration is often also called "inherent structure" (IS).[35,36] In practice, we have used a conjugate gradient algorithm[37] which is here a fast procedure since the system needs only to relax the thermal fluctuations without altering the connectivity of the system.

Within the harmonic approximation, the local minimum of V_{tot} can be written as a bilinear form in $\mathbf{q}$ and $\mathbf{q}$,

$$V'_{tot}(\mathbf{q}) = \frac{1}{2}\sum_{i=1}^{G}\sum_{j=1}^{G} \mathbf{q}\hat{\mathbf{H}}_{ij}\mathbf{q}, \tag{4}$$

where G is the number of degrees of freedom and

$$\hat{\mathbf{H}}_{ij} \equiv \left.\frac{\partial^2 V_{tot}(\mathbf{q})}{\partial q_i \partial q_j}\right|_{\mathbf{q}^*}. \tag{5}$$

The eigenvectors of the matrix $\hat{\mathbf{H}}_{ij}$ are the normal modes of our system and the square rooted eigenvalues are the eigenfrequencies. The normalized distribution of the latter is thus the vDOS $g(\omega)$.

To compute the Hessian $\hat{\mathbf{H}}_{ij}$ at the IS, we have used a finite difference method. Since bi-functional particles have patches located on the poles, only two angles are needed to identify the direction of the axis that joins them. This lowers the total number of degrees of freedom from $6N-3$ to $5N_2+6N_3-3$. The subsequent diagonalization was performed using the LAPACK package. To improve the statistics, we have averaged over $20-50$ configurations. Although these configurations are not independent (since they share the same network topology), this averaging significantly smooths the vDOS. We associate such improvement to sampling of the several secondary minima composing the same metabasin.[38]

III. RESULTS

A. Structure of the investigated systems

The networks studied in this article are composed by chains of bi-functional particles that are cross-linked by the three-functional particles, acting as hinges between the chains. Since bonds do not break during the time scale of the simulation, the system behaves as an almost fully connected chemical gel.[32] The possibility of tuning the concentration of junctions allows us to generate structures which have different chain lengths. Specifically, the average chain length, i.e., the average number of bi-functional particles between two three-functional ones (a length that is related to the average distance between branching points of the network) is given by[32]

$$\bar{l}=\frac{3-x_2}{3-3x_2}. \tag{6}$$

For the smallest value of x_2 studied here we have thus $\bar{l}\simeq 1.2$, while for the largest we obtain $\bar{l}=7.0$. The ability to predict theoretically $\bar{l}$ is made possible by the fact that the structure is essentially generated from an equilibrium configuration and hence can be quite accurately described by the theory of Flory and Stockmayer.[33,39]

To provide a visual representation of the networks generated for different values of the mean connectivity $\overline{M}$, we show in Fig. 1 two snapshots of the systems with $x_2=0.2$ and $x_2=0.9$, where the most mobile particles are highlighted.[40] From the figure we recognize that for x_2 small, i.e., high connectivity, the system seems to be more heterogeneous than if x_2 is large. This is due to the fact that in the former case the gas-liquid spinodal is closer to the investigated state point and thus fluctuations are larger.[32] Furthermore, we see that for small average connectivity the most mobile particles form chains, whereas for small x_2 their spatial distribution seems to be rather random. It is evident that the chain-like structure found at low connectivity will give rise to low frequency modes in the vDOS, and below we will discuss this in more detail.

B. Density of states

In this section, we discuss the density of states, calculated within the harmonic approximation, for different concentrations of bi-functional particles and correlate specific features of $g(\omega)$ with specific vibrational modes of the system.

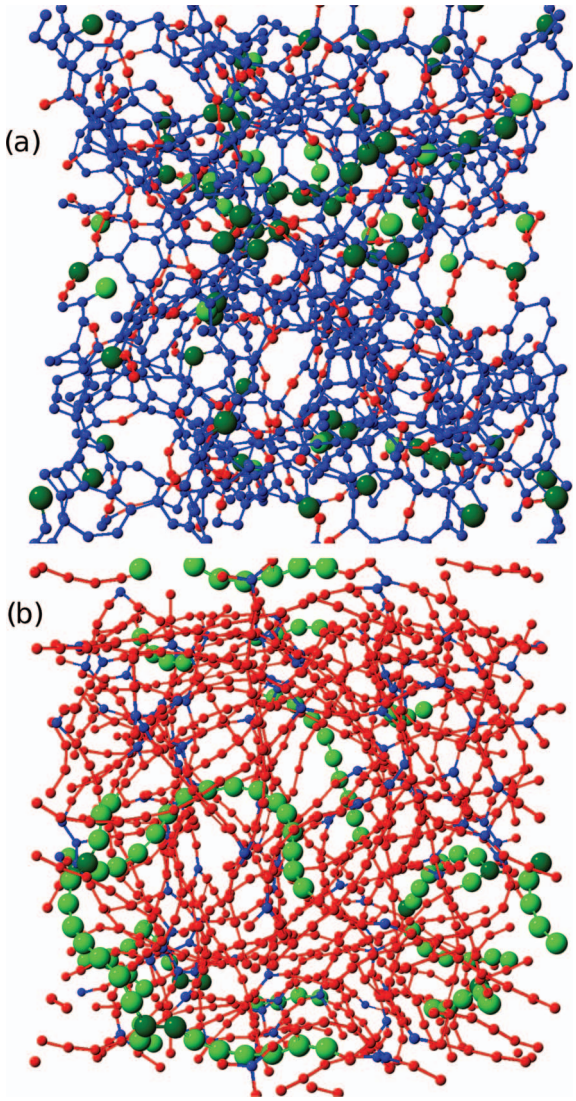

FIG. 1. A snapshot of the system at $T=0.04$ for $x_2=0.2$ (a) and $x_2=0.9$ (b). Small spheres: bi- and three-functional particles with low mobility (red and blue, respectively). Large spheres: bi- and three-functional particles with high mobility (light and dark green, respectively). A particle is defined to be mobile if it has a mean squared displacement >0.5 for $x_2=0.2$ and >7.0 for $x_2=0.9$.

The harmonic density of states for several values of $\overline{M}$ is shown in Fig. 2. For small x_2 the vDOS has one main peak at small frequencies and a tail that extents to high ω. With intermediate and large x_2 the vDOS displays two peaks, one located at $\omega\lesssim 0.38$ and one centered around $\omega\approx 1$, followed by a broad tail extending up to $\omega\approx 10$. Apart from the case $x_2=0.2$ (corresponding to $\bar{l}\approx 1.2$), which shows a clear decrease in the number of low frequency eigenmodes, no significant dependence on x_2 is observed in the fraction of modes contributing to the two main peaks and to the tail of the vDOS. This suggests that increasing the length of the chains does not strongly influence the total number of modes in the vDOS at low frequencies, but only the shape of $g(\omega)$. Indeed, with increasing x_2, the low frequency peak moves to lower frequencies and increases its height while the peak at intermediate frequencies becomes better resolved and a shoulder appears at $\omega\simeq 0.6$. For completeness, we note that a shoulder is also

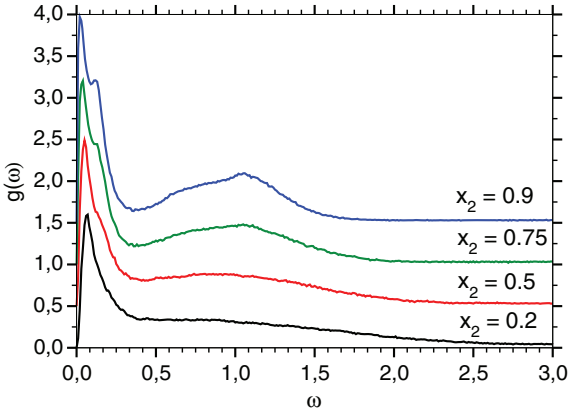

FIG. 2. Density of states $g(\omega)$ for different fractions of bi-functional particles x_2. At the lowest x_2 there is one peak and a long tail. With increasing x_2 a new peak appears while the minimum between the peaks becomes more pronounced but remains at the same position ($\omega_{min} \simeq 0.38$). Consecutive curves are shifted vertically by 0.5.

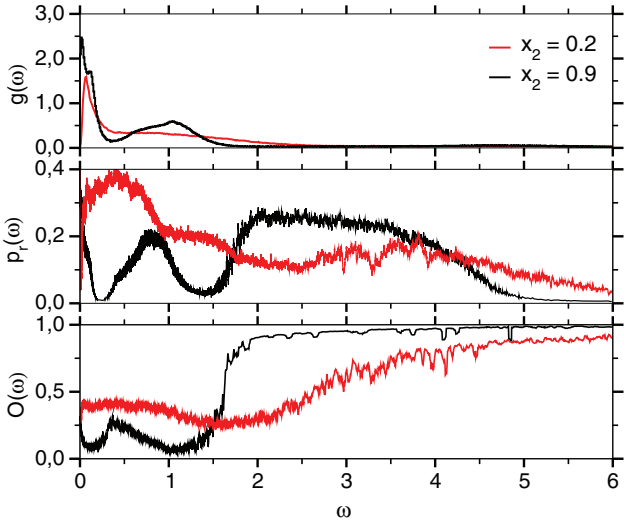

FIG. 3. $g(\omega)$ (top), $p_r(\omega)$ (middle), and $O(\omega)$ (bottom) for $x_2 = 0.2$ and $x_2 = 0.9$.

present in the low frequency peak ($\omega \simeq 0.1$), which turns into a minor peak when $x_2 = 0.9$.

Note that the peak at low ω is observed at frequencies that are significantly smaller than the *typical* frequencies of the model, which are on the order of unity (due to the choice of the units). Since the mentioned peak occurs at frequencies that are by a factor of 3–10 times smaller, we can tentatively identify this peak as a boson peak. From the figure we thus can conclude that there is a clear correlation between the *structure* of the system (open vs. compact network) and the height of the peak (high/low).

To better understand the nature of the oscillations in the different regions of the spectrum, we study the *participation ratio*, p_r, of each mode i. This quantity is defined as

$$p_r(\omega) = \left(N \sum_{n=1}^{N} \left| \mathbf{e}_i^n \right|^4 \right)^{-1}, \tag{7}$$

where $\mathbf{e}_i^n$ is the displacement vector of the nth particle of the ith normal mode. The participation ratio is a standard measure of localization of a mode.[42,43] For example, for a translation of the system $p_r(\omega) = 1$, while for a vibration of a single particle $p_r(\omega) = 1/N$.

In dense systems, the direction of the vibrations of a given particle, i.e., $\mathbf{e}_i^n$, is basically independent of the direction of the bonds that the particle forms with its neighbors. For a system that has long chains, as the one studied here, this is no longer the case and hence it is of interest to be able to discriminate between longitudinal and transverse modes with respect to the bond direction (i.e., along the local curvilinear direction of the chain). To this aim, we quantify to what extent the displacement of the ith normal mode is parallel to the local direction of the bond. By writing the direction joining bonded particles n and j as $\mathbf{v}_j^n \equiv \mathbf{r}_{nj}/r_{nj}$, the observable $O(\omega)$ is thus defined as

$$O(\omega) = \frac{1}{N} \sum_{n=1}^{N} \max_j \left| \mathbf{e}_i^n \cdot \mathbf{v}_j^n \right|^2, \tag{8}$$

where j is an index running over the bonded neighbors of particle n. Since $\mathbf{v}_j^n$ as well as $\mathbf{e}_i^n$ are normalized, $O(\omega) \in [0, 1]$. In the case of a unidimensional chain, a longitudinal mode has $O(\omega) = 1$ while a transverse one has $O(\omega) = 0$.

The functions $p_r(\omega)$ and $O(\omega)$ are shown in Fig. 3 for $x_2 = 0.2$ and $x_2 = 0.9$, together with the corresponding vDOS for an extended frequency range. On increasing x_2 both functions become more structured, suggesting that different frequency regions are populated by modes with different characteristics. We start by discussing the $x_2 = 0.9$ case. The data for $O(\omega)$ show that modes for $\omega > 1.5$, i.e., modes that are not in the two peaks seen in $g(\omega)$, have $O(\omega) \approx 1$, suggesting that such modes are mostly vibrations along the bond directions (reminiscent of longitudinal modes). In contrast to this, modes with $\omega < 1.5$ are characterized by a rather small value of $O(\omega)$, thus describing oscillations orthogonal to the chain direction, i.e., are similar to transverse modes. Note that the transition of $O(\omega) \approx 1$ to values ≤ 0.5 at $\omega \approx 1.5$ is quite sharp, indicating a well-defined crossover from longitudinal modes at high frequencies to transverse modes at low ω. The participation ratio, which never exceeds the value 0.4, suggests that all modes are mostly localized. We recall that the value usually taken as indication of a collective oscillation, i.e., of propagating phonons,[43] is $p_r \gtrsim 0.5$. Note that such propagating phonons are not even seen at low frequencies where one does expect acoustic modes. The absence of such excitations indicates that on the length scale of the simulation box the system is still very heterogeneous and as a consequence the modes cannot propagate. However, it can be expected that for larger simulation boxes such propagating modes will indeed be present and the rise of $p_r(\omega)$ at small ω can be taken as indication that one is approaching this acoustic regime. Also at values of ω in which $g(\omega)$ shows the peak around $\omega \approx 1.0$, we see that $p_r(\omega)$ is significantly larger than zero. Thus we conclude that also these modes show a significant delocalization. As we will show below, these modes correspond in fact to excitations in which a chain makes transverse oscillations, in agreement with the small values of $O(\omega)$

in this ω-range. Last but not least, we see that $p_r(\omega)$ is also relatively large if $\omega > 2.0$. This is (probably) related to the fact that at elevated frequencies the modes are a hybridization of (relatively) localized modes, thus should not really be considered as extended objects.[43]

In the case of $x_2 = 0.2$, $O(\omega)$ never reaches very small values and the difference between the region of the peaks and the tail is less pronounced. This indicates that even modes with $\omega < 3$ cannot be described to be transverse (with respect to the bond direction). This is consistent with the very short average chain length observed for small values of x_2. Furthermore, we see that $p_r(\omega)$ becomes relatively large as soon as $\omega \leq 1.0$, i.e., for these frequencies the modes are significantly more collective than for the case $x_2 = 0.9$. This is in agreement with the fact that for $x_2 = 0.2$, the structure of the system involves smaller length scales than the ones for large values of x_2 and hence acoustic-like modes can propagate even at relatively high frequencies. From $O(\omega)$, we also recognize that at large frequencies the modes appear to describe motion parallel to the bonds, i.e., $O(\omega)$ is large. Since the participation ratio is relatively small, this suggests that these longitudinal modes are localized. This feature is thus directly related to the structure of the system which, for small x_2, shows short rings of bonded particles, as displayed in Fig. 1(a).

To gain insight into the nature of the modes in the different regions of the spectrum, we compare the vDOS of the system with the vDOS of isolated elements of the network, found in the simulated configurations. In particular, we focus on three different structures: a bended chain of bi-functional particles, a star configuration in which three chains of bi-functional particles are connected via a central three-functional particle, and a ring of bi- and three-functional particles. The first two structures are typical elements for the network with large x_2, while the ring is relevant of the case with small x_2. Figure 4 shows the three selected structures, composed, respectively, of 18, 18, and 7 particles. The large number of particles in the first two structures allows us to explore a larger and better resolved range of frequencies. For the chain, the number of degrees of freedom and, therefore, the number of eigenvalues obtained is 92; for the star structure it is 94 and for the ring 38. We have also computed the density of states for chains whose length is comparable to the

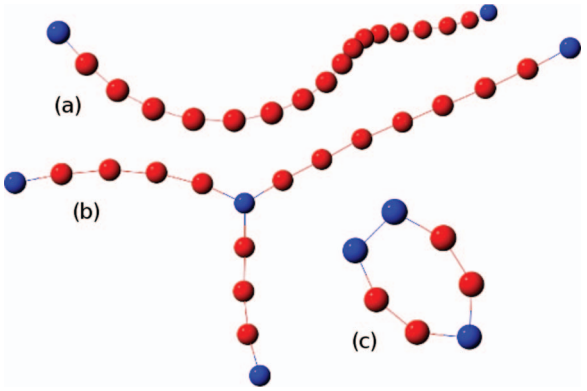

FIG. 4. Studied network elements: (a) A curved chain formed by 18 particles; (b) three chains linked together, 18 particles in total; (c) a closed ring. All these structures have been found in $x_2 = 0.9$ configurations at $T = 0.04$.

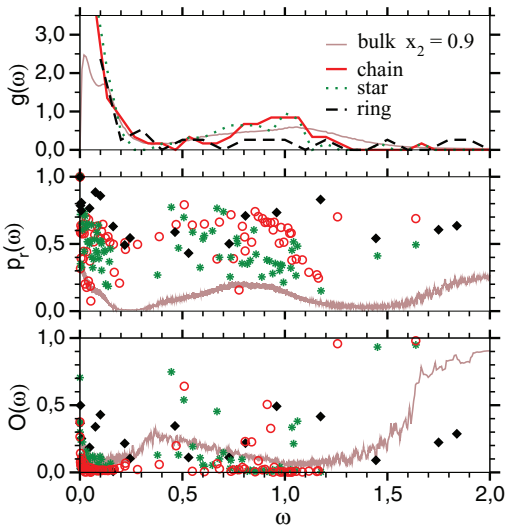

FIG. 5. $g(\omega)$ (top), $p_r(\omega)$ (middle), and $O(\omega)$ (bottom) for the structures pictured in Fig. 4: A ring (filled diamonds), a star of chains (stars), and a chain (open circles). For reference, we include also the $g(\omega)$, $p_r(\omega)$, and $O(\omega)$ of the entire system for $x_2 = 0.9$.

average chain length ($\bar{l} \simeq 7$) and we have obtained the same qualitative results.[41]

For each of these structures, we have computed the density of states after the usual minimization stage. The results are shown in Fig. 5. The chain and the star configurations have density of states that are remarkably similar to the one of the system with $x_2 = 0.9$. Instead, the ring's $g(\omega)$, is qualitatively more similar to the density of states of the system with $x_2 = 0.2$, i.e., it does not have a pronounced peak at $\omega \approx 1.0$. Figure 5 also shows the participation ratio and the $O(\omega)$ for the selected structures. Some of the features found in the bulk system are also observed in the eigenmodes of the examined structures, in that for $\omega > 1.5$, $O(\omega) \approx 1$ for the chain and the star while $O(\omega) \approx 0.2$ for the ring. Moreover, in the frequency region $\omega < 0.25$, both $O(\omega)$ as well as $p_r(\omega)$ are larger for the ring than for the chain and the star. Again these features are very similar to the ones found when analyzing the $x_2 = 0.2$ and $x_2 = 0.9$ systems. Hence, despite the small number of degrees of freedom of these structures, a strong correspondence with the features of the vDOS, of $O(\omega)$, and $p_r(\omega)$ of the bulk system can be found. Thus, the chain and star are indeed representative of the low valence network, while the ring is characteristic of the network rich in three-functional junctions.

As a consequence of the observed similarity between the chain and the $x_2 = 0.9$ system, we have the possibility to identify the different modes appearing in the vDOS. Figure 6 shows graphically the direction of the translational displacement of all particles belonging to the chain for characteristic frequencies that are located in different regions of the vDOS. One can identify the progression typical of one-dimensional chains on increasing frequency, even if the purity of the modes is significantly altered by the curvilinear structure. Indeed, the graphical inspection of the displacements, as well as the specific values of $p_r(\omega)$ and $O(\omega)$, consistently suggests a strong resemblance with a long wavelength acous-

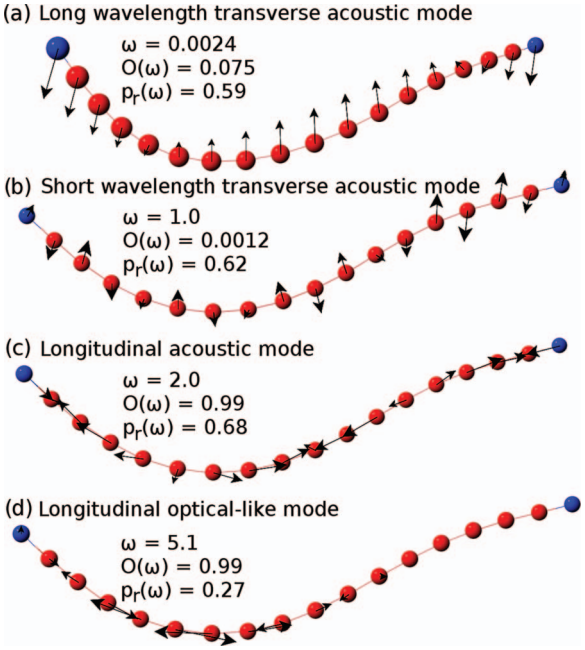

FIG. 6. Four characteristic vibrational modes of the bended chain.

tic transverse phonon (a), a short wavelength acoustic transverse phonon (b), a longitudinal acoustic phonon (c), and an optical-like longitudinal phonon (d). Of course, the curvilinear nature of the chain introduces some disorder that alters the purity of the modes.

Finally, we show in Fig. 7 three different modes of the ring, located in different frequency regions. Apart from the low frequency mode which has a large participation ratio, the other modes describe deformations of the structure. The different values of $O(\omega)$ indicate if the deformation takes place along the plane of the ring or if it is mostly perpendicular to it.

In order to further understand the origin of the peaks in the vDOS of our gel, it is useful to compare it to the one of a one-dimensional linear chain in the limit of very large N. For this, we have calculated the vDOS for a system of 1000 bi-functional particles located on a straight linear chain oriented in the $x$direction. Neighboring particles i

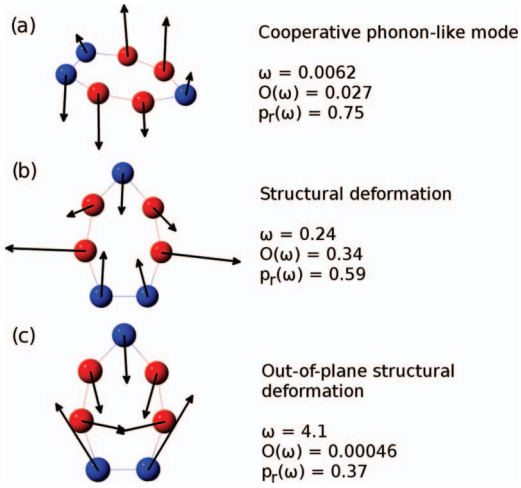

FIG. 7. Three characteristic vibrational modes of the ring.

and j are located at the distance corresponding to the minimum of $V(i, j)$, where $V(i, j)$ is the same inter-particle potential used in the simulation of the gel, see Eq. (1). The presence of angular degrees of freedom, which strongly couple to translational degrees of freedom, significantly alters the behavior of the vDOS with respect to the well-known textbook case of the one-dimensional chain of particles interacting only via harmonic springs.[1] To evaluate the role of the coupling, we first start by studying the corresponding system in which the coupling is missing. This is realized by setting for the diagonalization the translation-orientation blocks of the Hessian to zero.[44] Beside the translational and rotational vDOS, we have also investigated the dispersion relation, by analyzing the periodicity of the different eigenvectors. For this, we have calculated the space Fourier transform of each eigenvector and have associated the position of the peak in k-space to the corresponding eigenvalue ω. In the case of translation, motion along the chain direction provides information on the longitudinal branch, while displacements in the two orthogonal directions provide information on the transverse branches. Similarly, the periodicity of the two angular displacements of the particles along the chain provides information on the rotational modes. The dispersion relations and vDOS for the decoupled system are shown in the insets of Figs. 8(a) and 8(b). The longitudinal and transverse sound velocities v_l and v_t calculated from the slopes of the dispersion curves at small k (or equivalently from the square root of the second derivative of the potential with respect to the chain direction x for the longitudinal modes and with respect to y or z for the transverse ones) are found to be $v_l \simeq 2.24$ and $v_t \simeq 0.51$. The significantly smaller value of $\partial^2 V(i, j)/\partial y_i \partial y_j$ as compared to $\partial^2 V(i, j)/\partial x_i \partial x_j$ gives rise to a v_t that is much smaller than v_l and hence a transverse dispersion relation located at frequencies much smaller than the longitudinal one. This strong difference is plausible since it is much easier to deform the chain in its orthogonal direction than in its parallel direction. The translational vDOS of the system, inset of Fig. 8(b), shows a flat density of states, followed by a van Hove singularity around $\omega \approx 1$ (the boundary zone of the transverse band) and around $\omega \approx 4.5$ (the boundary of the longitudinal band, not shown in the figure). The rotational modes have an optical character in that they have, at $k = 0$, a finite frequency (inset of Fig. 8(a)). With increasing wave-vector the modes become softer, before they degenerate at the zone boundary.

Next, we come back to the original model, i.e., we include the coupling between translations and rotations when the Hessian is diagonalized. We see that this coupling induces strong changes in the dispersion relations, see main panel of Fig. 8(a). The coupling makes that there are now two transverse optical modes that at $k = 0$ have the frequency of the rotational modes of the uncoupled system. Similarly, the coupling makes that the rotational degrees of freedom can also have an acoustic branch, with a frequency at the zone boundary that is given by the ω of the uncoupled system. In contrast to the rotational and transverse modes, no significant change in the longitudinal excitations are seen. As a result of the coupling between the various modes, the vDOS at low ω becomes populated by modes which arise

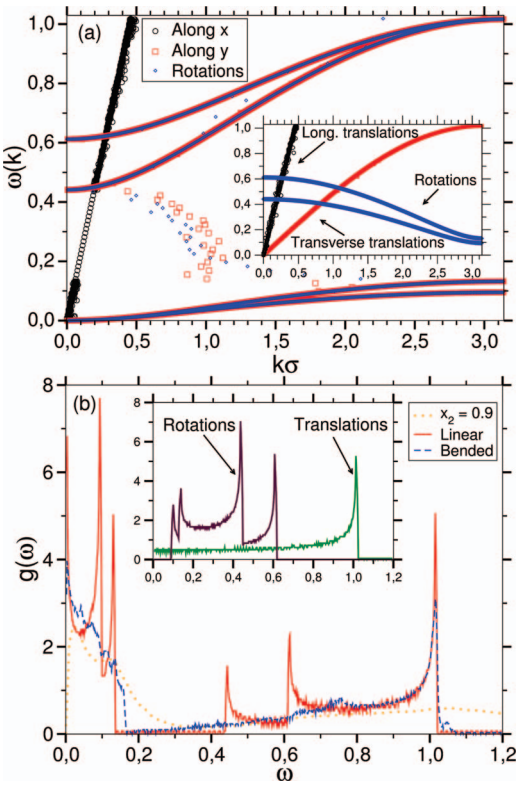

FIG. 8. (a) Dispersion relation for the linear chain, calculated by estimating the spatial periodicity along the x direction (longitudinal) and along the y or z (transverse) direction. The dispersion relations obtained by evaluating the periodicity for the two angles coincides with the y or z results, confirming the mixed nature of these modes. The inset shows the corresponding dispersion relation curves for the decoupled system in which we diagonalize only the $3N \times 3N$ block of the Hessian associated with translational degrees of freedom as well as the $2N \times 2N$ block associated with rotational degrees of freedom. (b) vDOS of a linear and of a bended chain of $N = 1000$ particles. The vDOS of the network with $x_2 = 0.9$ is also shown for comparison. The inset shows the vDOS calculated for the decoupled system. Note that the figure shows only the region $\omega < 1.2$ and; therefore, the van Hove singularity associated with the longitudinal modes and which is located at $\omega \approx 4.4$ is not visible.

from the strong coupling between the low frequency transverse translational modes and the optical rotational modes (Fig. 8(b)), thus explaining the presence of high intensity at low frequencies.

We have also calculated the vDOS of a long bended chain, and the results are also reported in Fig. 8(b). We see that the features of the linear chain are retained in the vDOS of the bended chain, even if the van-Hove singularities are now smeared out by the absence of linearity. Interestingly enough, the main features of the linear chain are also retained in the bulk system, whose broadbands can qualitatively associated with the linear chain bands, providing a strong support for the interpretation of the disordered network modes discussed previously (see Fig. 3).

IV. CONCLUSIONS

In this article, we have studied in detail the vDOS of a disordered system composed by poly-disperse chains of connected bi-functional particles, joined together via three-functional junctions. The relative concentration of bi- and three-functional particles makes it possible to control the average distance $\bar{l}$ between junctions and explore the effect of the network mesh on the vDOS.

We have found a clear evolution of the vDOS with $\bar{l}$, with a progressive structuring of $g(\omega)$. To provide a characterization of the modes in different frequency regions, we have calculated the participation ratio and the mode amplitude in the bond direction, which has allowed us to distinguish between localized and delocalized modes and transverse and longitudinal excitations. We have found support for the resulting classification via the analysis of specific structures of the networks, i.e., chains, stars of chains, and rings, finding that most of the features of the bulk vDOS can be associated with specific modes of these simpler structures.

We have also found very helpful the comparison with the vDOS of an infinite chain of particles interacting with the same potential. The comparison between the vDOS calculated in the presence and in the absence of rotational-translational coupling helps clarifying the importance of such a coupling and the nature of the bands observed in the bulk disordered network. In particular, we observed that the coupling between translations and rotations significantly increases the vDOS at low ω, which becomes populated by transverse modes, with frequencies which are strongly decreased (as compared to the uncoupled system) by the possibility of rotating the particles in coherence with the translational displacements. Interestingly, this band is clearly retained also in the vDOS of the bulk system.

This study suggests that properties of the disordered systems can partially be traced back to properties of the corresponding crystal, with an adequate smearing introduced by the absence of long-range periodicity and by the finite length of the chains. It also calls attention on the important role of the coupling between translations and rotations in the low frequency region of the spectrum, i.e., in the ω region where the boson peak is observed in glasses. *For the present model* it is this coupling that leads to a strong intensity of the vDOS at low frequencies. However, this mechanism to generate low-frequency modes is certainly not the only one since, i.e., disorder in the coupling constants or in the masses will also give rise to soft modes as has been shown for other systems.[17,18]

ACKNOWLEDGMENTS

We thank J. Russo for help during the initial stages of this work and A. V. Dobrynin and U. Buchenau for helpful discussions. L.R. and F.S. acknowledge support from ERC-226207-PATCHYCOLLOIDS and ITN-234810-COMPLOIDS. W.K. is a senior member of the Institut universitaire de France.

[1] N. W. Ashcroft and N. D. Mermin, *Solid State Physics* (Brooks-Cole, New York, 1976).
[2] H. Kuzmany, *Solid-State Spectroscopy: An Introduction* (Springer, Berlin, 2002).
[3] S. Alexander and R. Orbach, J. Phys. (Paris), Lett. **43**, L625 (1982).
[4] R. Rammal and G. Toulouse, J. Phys. (Paris), Lett. **44**, L13 (1983).
[5] E. Courtens, J. Pelous, J. Phalippou, R. Vacher, and T. Woignier, Phys. Rev. Lett. **58**, 128 (1987); E. Courtens, R. Vacher, J. Pelous, and T. Woignier, Europhys. Lett. **6**, 245 (1988); P. Benassi, M. Krisch, C. Masciovecchio, V. Mazzacurati, G. Monaco, G. Ruocco, F. Sette, and R. Verbeni, Phys. Rev. Lett. **77**, 3835 (1996).

[6]U. Buchenau, N. Nücker, and A. J. Dianoux, Phys. Rev. Lett. **53**, 2316 (1984).
[7]A. P. Sokolov, E. Rössler, A. Kisliuk, and D. Quitmann, Phys. Rev. Lett. **71**, 2062 (1993).
[8]S. N. Taraskin and S. R. Elliott, Phys. Rev. B **56**, 8605 (1997).
[9]E. Courtens, M. Foret, B. Hehlen, and R. Vacher, Solid State Commun. **117**, 181 (2001).
[10]J. Horbach, W. Kob, and K. Binder, Eur. Phys. J. B **19**, 531 (2001).
[11]T. Theenhaus, R. Schilling, A. Latz, and M. Letz, Phys. Rev. E **64**, 051505 (2001).
[12]T. Nakayama, Rep. Prog. Phys. **65**, 1195 (2002).
[13]E. Courtens, M. Foret, B. Hehlen, B. Rufflé, and R. Vacher, J. Phys.: Condens. Matter **15**, S1279 (2003).
[14]M. Wyart, S. R. Nagel, and T. A. Witten, Europhys. Lett. **72**, 486 (2005).
[15]W. Schirmacher, Europhys. Lett. **73**, 892 (2006).
[16]B. Rufflé, D. A. Parshin, E. Courtens, and R. Vacher, Phys. Rev. Lett. **100**, 015501 (2008).
[17]B. Schmid and W. Schirmacher, Phys. Rev. Lett. **100**, 137402 (2008).
[18]V. Ilyin, I. Procaccia, I. Regev, and Y. Shokef, Phys. Rev. B **80**, 174201 (2009).
[19]K. Binder and W. Kob, *Glassy Materials and Disordered Solids: An Introduction to their Statistical Mechanics*, 2nd ed. (World Scientific, Singapore, 2011).
[20]H. Shintani and Tanaka, Nature Mater. **7**, 870 (2008).
[21]D. Engberg, A. Wischnewski, U. Buchenau, L. Börjesson, A. J. Dianoux, A. P. Sokolov, and L. M. Torell, Phys. Rev. B **56**, 4053 (1999).
[22]V. N. Novikov, Y. Ding, and A. P. Sokolov, Phys. Rev. E **71**, 061501 (2005).
[23]W. A. Kamitakahara, R. L. Cappelletti, P. Boolchand, B. Halfpap, F. Gompf, D. A. Neumann, and H. Mutka, Phys. Rev. B **44**, 94 (1991).
[24]E. Zaccarelli, J. Phys.: Condens. Matter **19**, 323101 (2007).
[25]E. Zaccarelli, S. V. Buldyrev, E. La Nave, A. J. Moreno, I. Saika-Voivod, F. Sciortino, and P. Tartaglia, Phys. Rev. Lett. **94**, 218301 (2005).
[26]E. Del Gado and W. Kob, Europhys. Lett. **72**, 1032 (2005).
[27]E. Bianchi, J. Largo, P. Tartaglia, E. Zaccarelli, and F. Sciortino, Phys. Rev. Lett. **97**, 168301 (2006).
[28]R. Blaak, M. A. Miller, and J.-P. Hansen, Europhys. Lett. **78**, 26002 (2007).
[29]S. Saw, N. L. Ellegaard, W. Kob, and S. Sastry, Phys. Rev. Lett. **103**, 248305 (2009).
[30]J. Russo, M. Tavares, P. I. C. Teixeira, M. M. Telo da Gama, and F. Sciortino, Phys. Rev. Lett. **106**, 085703 (2011).
[31]E. Zaccarelli, I. Saika-Voivod, S. V. Buldyrev, A. J. Moreno, P. Tartaglia, and F. Sciortino, J. Chem. Phys. **124**, 124908 (2006).
[32]J. Russo, P. Tartaglia, and F. Sciortino, J. Chem. Phys. **131**, 014504 (2009).
[33]E. Bianchi, P. Tartaglia, E. La Nave, and F. Sciortino, J. Phys. Chem. B **111**, 11765 (2007).
[34]E. Bianchi, P. Tartaglia, E. Zaccarelli, and F. Sciortino, J. Chem. Phys. **128**, 144504 (2008).
[35]F. H. Stillinger and T. A. Weber, Science **225**, 983 (1984).
[36]F. Sciortino, J. Stat. Mech.: Theory Exp. **5**, 15 (2005).
[37]W. H. Press, B. P. Flannery, S. A. Teukolsky, and W. T. Vetterling, *Numerical Recipes in Fortran* (Cambridge University Press, New York, 1999).
[38]A. Heuer, J. Phys.: Condens. Matter **20**, 373101 (2008).
[39]P. J. Flory, *Principles of Polymer Chemistry* (Cornell University, London, 1953).
[40]In order to define the mobility of a particle we have calculated the mean squared displacement for each particle and generated the corresponding histogram. Note that this mean squared displacement is bounded, since bonds do not break. We found that this distribution has a very sharp peak at small displacements and a long tail at large displacements (Ref. 41).
[41]L. Rovigatti, M.S. thesis, Università di Roma "La Sapienza," 2009.
[42]B. B. Laird and H. R. Schober, Phys. Rev. Lett. **66**, 636 (1991).
[43]H. R. Schober and C. Oligschleger, Phys. Rev. B **53**, 11469 (1996).
[44]F. Sciortino and S. Sastry, J. Chem. Phys. **100**, 3881 (1994).